

# Design of a Jerusalem-Cross Slot Antenna for Wireless Internet Applications

Shu-Huan Wen and Hsing-Yi Chen

Department of Communications Engineering  
Yuan Ze University, Chung-Li, Taoyuan, 32003, Taiwan  
s1058603@mail.yzu.edu.tw, eehychen@saturn.yzu.edu.tw

**Abstract** — This paper provides a fast solution for the design of a Jerusalem-cross slot antenna for arbitrarily specifying any two operating frequencies. From simulation data and measurement results, the dual-resonant frequencies of the Jerusalem-cross slot antenna are found at near 5.8 and 24.0 GHz for the impedance matching with better than 15 dB return loss. It is found that the simulated and measured -10 dB bandwidths are 22.1% and 24.4% at 5.8 GHz respectively. The simulated and measured -10 dB bandwidths are 3.41% and 4.58% at 24.0 GHz, respectively. The simulated and measured results of radiation patterns in the E- and H-plane at frequencies of 5.8 and 24.0 GHz are broad and smooth. The antenna gains obtained by measurement and simulation at frequencies of 5.8 and 24.0 GHz are close to 3.0 and 6.0 dBi, respectively. This Jerusalem-cross slot antenna has a compact size with three dimensions of  $22.731 \times 7.577 \times 0.87$  mm which can be fabricated at a low cost using the standard PCB process. The compact patch antenna is suitable for applications in unlicensed frequency bands of 5.8 and 24 GHz for wireless internet applications including RFID systems, medical devices, and the internet of things (IoT).

**Index Terms** — Antenna gain, dual-resonant frequencies, Jerusalem-cross frequency selective surface, radiation pattern,

## I. INTRODUCTION

Recently, the internet of things (IoT) is a booming market. Under the concept of IoT, tens of billions of devices and systems can be connected via wireless technologies [1]. The IoT can be widely applied in healthcare, utility, media, transportation, environment and energy management, exploration, and smart homes/cities. Its demand for incorporating with wireless technologies is increasing. This will increase the demand for IoT antennas compliant to IoT modules. The type and number of wireless technologies used in IoT will impact the type and number of antennas needed. Since an IoT module should be designed as compact as possible, the corresponding system board sizes and antenna volume should be miniaturized to form miniaturized sensors that

meet versatile IoT needs. The types of IoT antennas may be chip antennas, wire antennas, whip antennas, or patch antennas.

Patch antennas have many advantages including low profile, low weight, low cost, and easy fabrication. Nevertheless, a patch antenna also has many drawbacks such as narrow band, low gain, low efficiency, poor polarization purity, and limited power capacity. Many researchers extend great effort to overcome these drawbacks in order to make full use of the advantages of a patch antenna. These efforts include selecting suitable substrate, changing the patch antenna's shape and size, using a variety of feeding techniques, application of impedance matching methods, using stacked layer structures, and the implementation of frequency selective surfaces [2-19].

Frequency selective surface (FSS) has a wide variety of applications including the design of antennas [17-31]. The FSS is usually formed by periodic arrays of metallic patches or slots of arbitrary geometries. The patch type FSS is used where reflection is maximum at resonant frequencies, while the slot type FSS is used where transmission is maximum at resonant frequencies. The FSS structure has a phenomenon with high impedance surfaces that reflect the plane wave in-phase and suppress surface waves. Therefore, a patch antenna with one FSS structure can improve its radiation efficiency, bandwidth, gain, and reduce the side lobe and back lobe level in its radiation pattern [17], [18], [32].

In this study, the frequency bands of 5.8 and 24.0 GHz are chosen for designing a Jerusalem-cross slot antenna based on frequency selective surface (FSS). We consider the WiFi frequency range at 5.8 GHz for this study because it is an unlicensed use and may be used for wireless internet applications including RFID systems and IoT. Recently, the 24.0 GHz frequency has been proposed by several authors from industry and academia [33-35] for wireless internet applications. The 24.0 GHz industrial, scientific, and medical (ISM) frequency band is of wide interest because unlicensed devices and services are permitted and the atmospheric attenuation does not compromise the communication [36].

Based on a dual-band Jerusalem-cross FSS with a

Rogers RO4003 substrate on one side, a compact Jerusalem-cross slot antenna is designed for wireless internet applications operating at 5.8 and 24.0 GHz. Return losses, radiation patterns, and antenna gains of the Jerusalem-cross slot antenna at 5.8 and 24.0 GHz are presented in this paper. Comparison of antenna performance between measurement results and HFSS (Ansoft, Pittsburgh, PA) simulation data is also made.

## II. ANTENNA DESIGN

Based on previous research works [37-38], we can quickly obtain optimum values of geometrical parameters of a dual-band Jerusalem-cross FSS with a Rogers RO4003 substrate operating at two resonant frequencies of 5.8 and 24.0 GHz in 20.66 seconds. Figure 1 shows the Jerusalem-cross FSS with a Rogers RO4003 substrate on one side and its optimum values of geometrical parameters  $p$ ,  $w$ ,  $s$ ,  $h$ ,  $d$ ,  $t$  and  $T$ . In Fig. 1,  $p = 7.577$  mm is the periodicity of a unit cell,  $w = 0.6059$  mm is the width of the conductive strip,  $s = 0.1294$  mm is the separation distance between adjacent units,  $h = 0.3793$  mm is the width of the end caps of the Jerusalem-cross,  $d = 4.931$  mm is the length of the end caps of the Jerusalem-cross,  $t = 0.035$  mm is the thickness of the metallic foil, and  $T = 0.8$  mm is the thickness of the Rogers RO4003 substrate. The relative dielectric constant and dielectric loss tangent of the Rogers RO4003 substrate are  $\epsilon_r = 3.31$  and  $\tan\delta = 0.0027$ , respectively. Figure 2 shows the frequency response of transmission of the Jerusalem-cross FSS with the Rogers RO4003 substrate on one side obtained by a HFSS simulator. It is clear that resonant frequencies of this patch FSS can be found very close to 5.8 and 24.0 GHz, respectively.

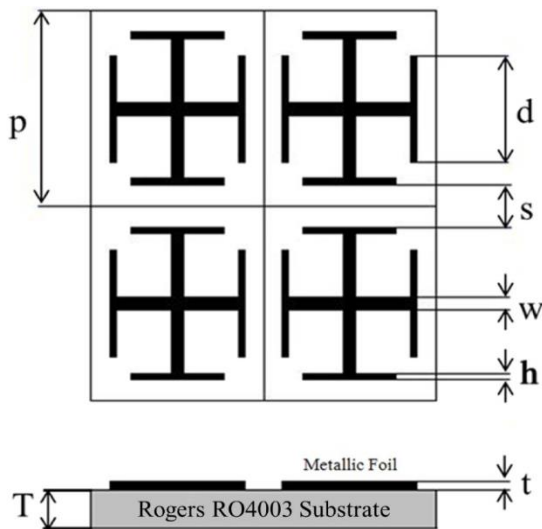


Fig. 1. A Jerusalem-cross FSS with a Rogers RO4003 substrate on one side operating at 5.8 and 24.0 GHz.

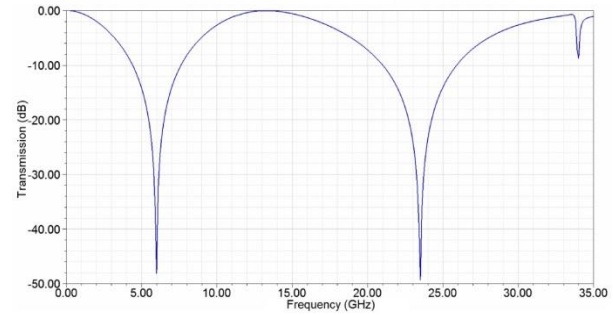


Fig. 2. Frequency response of transmission of the dual-band Jerusalem-cross FSS with a Rogers RO4003 substrate on one side.

For a slot FSS, it is designed where transmission is maximum but reflection is minimum in the neighborhood of the resonant frequency. In designing a Jerusalem-cross slot antenna, a complementary patch FSS (slot FSS) with a Rogers RO4003 substrate on one side is used as the radiator of the antenna. Figure 3 shows a Jerusalem-cross slot antenna with an off-center feeding to excite dual resonant frequencies of 5.8 and 24.0 GHz. This antenna has a compact size with dimensions of  $22.731 \times 7.577 \times 0.87$  mm. The same geometrical parameters of the patch FSS as shown in Fig. 1 are used to construct the slot FSS of this antenna. This antenna is designed on a single layer Rogers PCB board with a relatively big ground plane. The ground plane of this antenna would change the radiation performance, especially, the radiation pattern. A 50-ohm micro-strip feeding line having a length of  $L=P/2$  and a width of 1 mm is used to excite the antenna with an SMA connector attached on the ground plane. Frequency response of reflection coefficient ( $S_{11}$ ) of this antenna obtained by HFSS simulations is shown in Fig. 4. From Fig. 4, it is clear that the lower resonant frequency of 5.8 GHz is well matched below -10 dB in the simulation. However, unsatisfied matching is observed: the higher resonant frequency of 24 GHz is not well matched below -10 dB. For IoT applications, at least -10 dB matching is usually required. Therefore, it is needed to fine tune the geometrical parameters of this antenna to overcome the unsatisfied matching problem at 24.0 GHz.

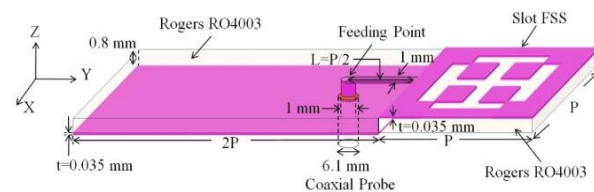


Fig. 3. The Jerusalem-cross slot antenna. The copper foil is in pink.

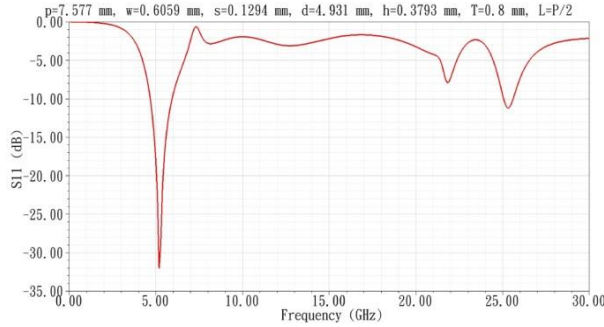


Fig. 4. Frequency response of return loss (S11) of the antenna.

In order to improve the reflection coefficient at 24 GHz, a few new optimum values of geometrical parameters of a dual-band Jerusalem-cross FSS with a Rogers RO4003 substrate are tuned by arbitrarily specifying any two resonant frequencies of 5.8 and  $24.0 \pm (0.01 \sim 0.5)$  GHz [37-38]. The fine-tuned geometrical parameters of the slot FSS are found to be  $p = 7.426$  mm,  $w = 1.076$  mm,  $s = 0.8693$  mm,  $h = 0.467$  mm, and  $d = 4.931$  mm. Frequency response of reflection coefficient (S11) of the fine-tuned antenna is shown in Fig. 5. From Fig. 5, it is shown that two resonant frequencies of 5.8 and 24.0 GHz are well matched below -10 dB in HFSS simulations. It is also shown that an undesired frequency band of 19.0 GHz appears in the frequency response. In the HFSS software computer program, current distributions on the antenna surface can be simulated and presented at any frequency. In order to eliminate the undesired frequency band, the current distribution of the fine-tuned antenna at 19.0 GHz is checked and presented in Fig. 6. It is clear that higher current densities are located at the right hand side of the fine-tuned antenna at 19.0 GHz. In the final design step, two half cylinders in the left hand side of the FSS are removed to eliminate the radiation source at 19.0 GHz and the Jerusalem-cross slot antenna is reconstructed as shown in Fig. 7. In Fig. 7, the ground plane and the FSS are separated by a distance of 0.4 mm and the length of the FSS is extended by 0.1 mm. The length of the ground plane is shortened from  $2P$  to  $1.8P$ . The length and width of the 50-ohm micro-strip feeding line are changed to  $L = P/2 - 0.1$  mm and 1.524 mm, respectively. Frequency responses of reflection coefficient (S11) of the final Jerusalem-cross slot antenna obtained by simulation and measurement are shown in Fig. 8.

From Fig. 8, the undesired frequency band of 19.0 GHz is improved and the resonant frequencies of the patch antenna are found to be near 5.8 and 24.0 GHz for the impedance matching with better than 15 dB return loss. Return losses of 24.5 and 28.5 dB are achieved by the measurements and simulations at 5.8 GHz, respectively. On the other hand, return losses of 40.9 and 16.0 dB

are achieved by the measurements and simulations at 24.0 GHz, respectively. It is found that the bandwidths for 10 dB return loss obtained by the HFSS simulations are 22.1% and 3.41% at resonant frequencies of 5.8 and 24.0 GHz respectively. It is also found that the bandwidths for 10 dB return loss obtained by the measurements are 24.4% and 4.58% at resonant frequencies of 5.8 and 24.0 GHz, respectively. It is clear that this Jerusalem-cross slot antenna provides a very wide bandwidth at 5.8 GHz. Instead of having a wide bandwidth at 5.8 GHz, the bandwidth of 3.41~4.58% occurring at 24.0 GHz is much narrower. The prototype of the Jerusalem-cross slot antenna is shown in Fig. 9. From Fig. 9, it is shown that this Jerusalem-cross slot antenna has a compact size with three dimensions of  $22.731 \times 7.577 \times 0.87$  mm.

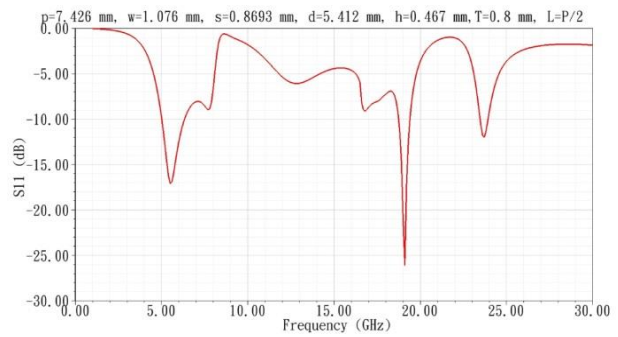


Fig. 5. Frequency response of reflection coefficient (S11) of the fine-tuned antenna.

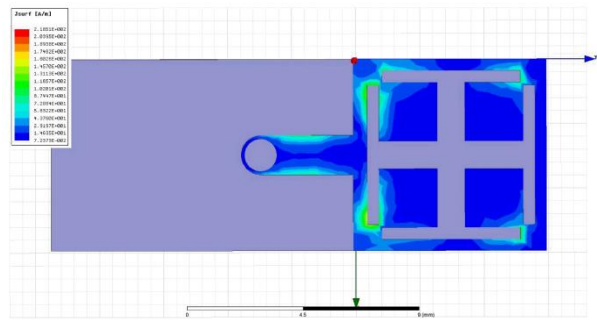


Fig. 6. Current distribution of the fine-tuned antenna at 19 GHz.

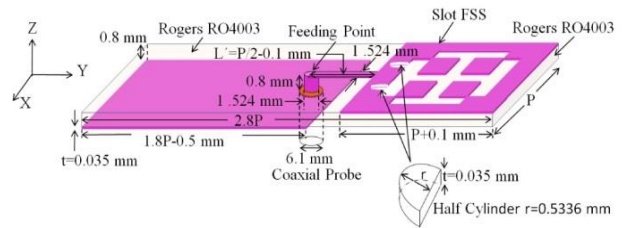


Fig. 7. The final structure of the Jerusalem-cross slot antenna. The copper foil is in pink.

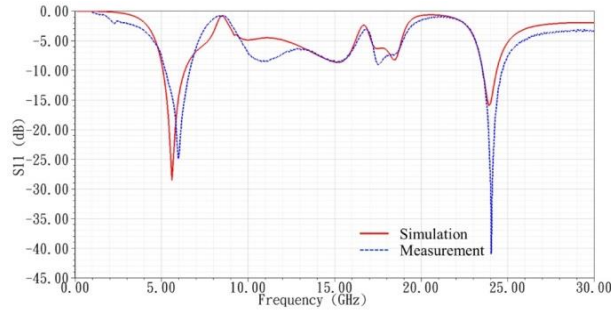


Fig. 8. Frequency response of reflection coefficient ( $S_{11}$ ) of the final Jerusalem-cross slot antenna.

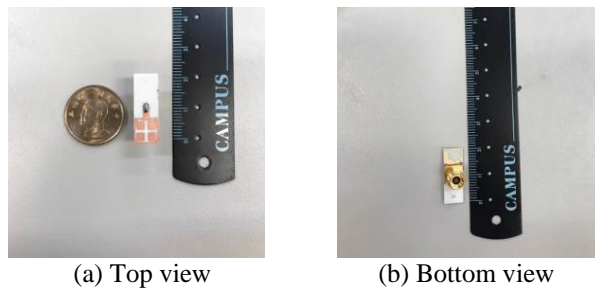


Fig. 9. Prototype of the Jerusalem-cross slot antenna.

### III. MEASUREMENT AND SIMULATION OF ANTENNA PERFORMANCE

Measurement results and simulation data of antenna performance were obtained by using an Anritsu37369C antenna measurement system in the Yuan Ze University (YZU) anechoic chamber and by using the HFSS simulator, respectively. Measurement setup in the YZU anechoic chamber is shown in Fig. 10. Comparisons of 3-D and 2-D radiation patterns between simulation data and measurement results at 5.8 and 24.0 GHz are shown in Figs. 11-16. It can be observed that the pattern shape and beam angle obtained by the simulation and measurement are similar to each other. The radiation patterns in the E- and H-plane are broad and smooth. Radiation patterns shown in Figs. 12, 13, 15, and 16 are presented both for a co-polarization and a cross-polarization response. In general, the co-polarization is the desired polarization for an antenna design. Due to the depolarization mechanisms, a polarization orthogonal to co-polarization called cross-polarization will be generated in an antenna radiation pattern. The polarization quality is expressed by the ratio of co-polarization to cross-polarization. The averaged ratio between co-polarization and cross-polarization shown in Figs. 12 and 13 is greater than 20 dB. This indicates that the system power loss due to polarization mismatch is insignificant at 5.8 GHz. The averaged ratio between co-polarization and cross-polarization shown in Fig. 16 is also greater than 20 dB,

but the averaged ratio between co-polarization and cross-polarization shown in Fig. 15 is much less than 20 dB. This means that the system power loss due to polarization mismatch may be significant at 24.0 GHz. The antenna gains obtained by simulation and measurement are shown in Table 1. The antenna gains obtained by simulation are 2.75 and 5.89 dBi at 5.8 and 24.0 GHz, respectively. The antenna gains obtained by measurement are 3.07 and 6.11 dBi at 5.8 and 24 GHz, respectively. From Figs. 11-16 and Table 1, it is shown that simulation data and measurement results make a good agreement in radiation patterns and antenna gains. This Jerusalem-cross slot antenna demonstrates a good example of dual-resonance operation at 5.8 and 24.0 GHz.

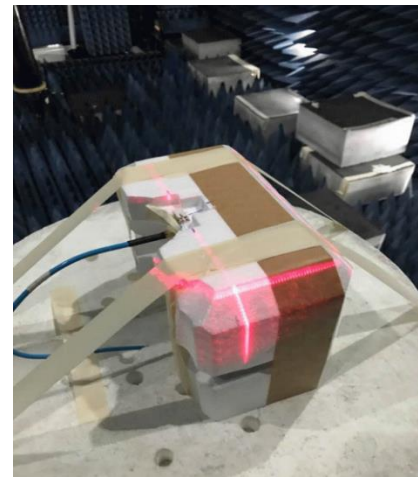
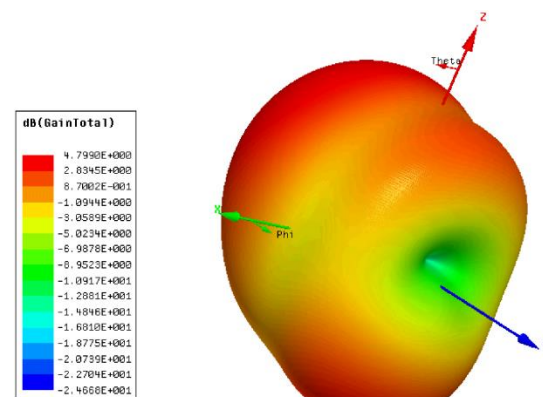


Fig. 10. Measurement setup in the YZU anechoic chamber.

Table 1: Antenna gain at 5.8 and 24.0 GHz

Frequency	5.8 GHz	24 GHz
Simulated (dBi)	2.75	5.89
Measured (dBi)	3.07	6.11



(a) Simulation



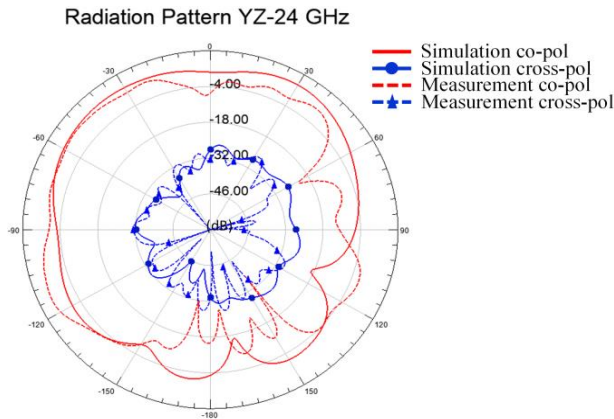


Fig. 16. Comparison of radiation patterns between simulation data and measurement results in the H-plane (y-z plane) at 24.0 GHz.

#### IV. CONCLUSIONS

Based on the studies of dual-band Jerusalem-cross frequency selective surface with substrates, we can quickly design a compact Jerusalem-cross slot antenna for WiFi and medical applications. The design procedure is presented in this paper. Measurement results and simulation data of antenna properties were obtained by using an Anritsu37369C antenna measurement system in the YZU anechoic chamber and by using the Ansoft high-frequency structure simulator (HFSS), respectively. It is shown that simulation data and measurement results make a good agreement in antenna properties. The dual-resonant frequencies of this patch antenna are found at near 5.8 and 24.0 GHz for the impedance matching with better than 15 dB return loss. It is found that the simulated -10 dB bandwidths are 22.1% and 3.41% at 5.8 and 24 GHz respectively. The measured -10 dB bandwidths are 24.4% and 4.58% at 5.8 and 24.0 GHz, respectively. It is clear that this Jerusalem-cross slot antenna provides a very wide bandwidth at 5.8 GHz. Broad and smooth radiation patterns are found in the E- and H-plane. The antenna gains obtained by measurement and simulation at frequencies of 5.8 and 24.0 GHz are close to 3.0 and 6.0 dBi, respectively. This compact patch antenna has three dimensions of  $22.731 \times 7.577 \times 0.87$  mm which can be fabricated at a low cost using the standard PCB process. Finally, this compact patch antenna can be used to apply in unlicensed frequency bands of 5.8 and 24.0 GHz for wireless internet applications including RFID systems, medical devices, and IoT.

#### REFERENCES

- [1] D. Evans, *The Internet of Things: How the Next Evolution of the Internet Is Changing Everything*, White Paper, Apr. 2011 [Online]. Available: [https://www.cisco.com/c/dam/en\\_us/about/ac79/docs/innov/IoT\\_IBSG\\_0411FINAL.pdf](https://www.cisco.com/c/dam/en_us/about/ac79/docs/innov/IoT_IBSG_0411FINAL.pdf)
- [2] K. L. Wong and K. P. Yang, "Compact dual frequency microstrip antenna with a pair of bend slot," *Electronic Lett.*, vol. 34, pp. 225-226, 1988.
- [3] P. C. Prasad and N. Chattoraj, "Design of compact Ku band microstrip antenna for satellite communication," *Communications and Signal Processing (ICCSPP), 2013 International Conference*, pp. 196-200, Apr. 3-5, 2013.
- [4] R. Q. Lee, K. F. Lee, and J. Bobinchak, "Characteristics of a two-layer electromagnetically coupled rectangular patch antenna," *Electron. Lett.*, vol. 23, pp. 1070-1072, 1987.
- [5] M. Rubelj, P. F. Wahid, and C. G. Christodoulou, "A microstrip antenna array for direct broadcast satellite receivers," *Microw. Opt. Technol. Lett.*, vol. 15, no. 2, pp. 68-72, 1997.
- [6] B. L. Ooi, "A double-II stub proximity feed U-slot patch antenna," *IEEE Trans. Antennas Propag.*, vol. 52, no. 9, pp. 2491-2496, Sep. 2004.
- [7] R. Chair, C. L. Mak, K. F. Lee, K. M. Luk, and A. Kishk, "Miniature wide-band half U-slot and half E-shaped patch antenna," *IEEE Trans. Antennas Propag.*, vol. 53, no. 8, pp. 2645-2652, Aug. 2005.
- [8] U. H. Park, H. S. Noh, S. H. Son, K. H. Lee, and S. I. Jeon, "A novel mobile antenna for Ku-band satellite communications," *ETRI J.*, vol. 27, no. 3, pp. 243-249, 2005.
- [9] R. Saluja, et al., "Analysis of bluetooth patch antenna with different feeding techniques using simulation and optimization," in *Proc. International Conference on Recent Advances in Microwave Theory and Applications*, pp. 742-744, 2008.
- [10] V. V. Reddy and R. Rana, "Design of linearly polarized rectangular microstrip patch antenna using IE3D/PSO," Bachelor thesis, Department of Electronics and Communication Engineering, National Institute of Technology Rourkela, Rourkela, 2009.
- [11] U. K. Revankar and A. Kumar, "Broadband stacked three-layer circular microstrip antenna arrays," *Electron. Lett.*, vol. 28, no. 21, pp. 1995-1997, 1992.
- [12] E. Nishiyama, S. Egashira, and A. Sakitani, "Stacked circular polarized microstrip antenna with wide band and high gain," *Proc. IEEE AP-S Int. Symp. and URSI Radio Science Meeting*, pp. 1923-1926, 1992.
- [13] S. Egashira, E. Nishiyama, and A. Sakitani, "Stacked microstrip antenna with wide band and high gain," *IEEE Trans. Antennas Propag.*, vol. 44, no. 11, pp. 1533-1534, 1996.
- [14] H.-S. Noh and U.-H. Park, "Three-stacked microstrip patch array antenna for both transmitting and receiving," *IEE Proc.-Microw. Antennas Propag.*, vol. 153, no. 4, pp. 385-388, Aug. 2006.
- [15] K. Agarwal, Nasimuddin, and A. Alphones, "Triple-

- band compact circularly polarised stacked microstrip antenna over reactive impedance meta-surface for GPS applications," *IET Microw. Antennas Propag.*, vol. 8, no. 13, pp. 1057-1065, 2014.
- [16] Y. Gao, R. Ma, Y. Wang, Q. Zhang, and C. Parini, "Stacked patch antenna with dual-polarization and low mutual coupling for massive MIMO," *IEEE Trans. Antennas Propag.*, vol. 64, no. 10, pp. 4544-4549, Oct. 2016.
- [17] H. Y. Chen and Y. Tao, "Bandwidth enhancement of a U-Slot patch antenna using dual-band frequency selective surface with double rectangular ring elements," *Microw. Opt. Technol. Lett.*, vol. 53, no. 7, pp. 1547-1553, July 2011.
- [18] H. Y. Chen and Y. Tao, "Performance improvement of a U-slot patch antenna using a dual-band frequency selective surface with modified Jerusalem cross elements," *IEEE Trans. Antennas Propag.*, vol. 59, no. 9, pp. 3482-3486, Sep. 2011.
- [19] D. Nashaat, H. A. Elsadek, E. A. Abdallah, M. F. Iskander, and H. M. El Hennawy, "Ultrawide bandwidth 2 2 microstrip patch array antenna using electromagnetic band-gap structure (EBG)," *IEEE Trans. Antennas Propag.*, vol. 59, no. 5, pp. 1528-1534, May 2011.
- [20] B. A. Munk, R. J. Luebbers, and R. D. Fulton, "Transmission through a 2-layer array of loaded slots," *IEEE Trans. Antennas Propag.*, vol. AP22, no. 6, pp. 804-809, Nov. 1974.
- [21] M. A. Hiranandani, A. B. Yakovlev and A. A. Kishk, "Artificial magnetic conductors realized by frequency-selective surfaces on a grounded dielectric slab for antenna applications," *IEE Pro.-Microw. Antennas Propag.*, vol. 153, no. 5, pp. 487-493, Oct. 2006.
- [22] F. Yang and Y. Rahmat-Samii, "Reflection phase characterizations of the EBG ground plane for low profile wire antenna applications," *IEEE Trans. Antennas Propag.*, vol. 51, no. 10, pp. 2691-2703, Oct. 2003.
- [23] J. Liang and H. Y. David Yang, "Radiation characteristics of a microstrip patch over an electromagnetic bandgap surface," *IEEE Trans. Antennas Propag.*, vol. 55, no. 6, pp. 1691-1697, June 2007.
- [24] D. Sievenpiper, L. Zhang, R. F. Jimenez Broas, N. G. Alex'opolous, and E. Yablonovitch, "High-impedance electromagnetic surfaces with a forbidden frequency band," *IEEE Trans. Microwave Theory Tech.*, vol. 47, no. 11, pp. 2059-2074, Nov. 1999.
- [25] Y. Zhang, J. von Hagen, M. Younis, C. Fischer, and W. Wiesbeck, "Planar artificial magnetic conductors and patch antennas," *IEEE Trans. Antennas Propag.*, vol. 51, no. 10, pp. 2704-2712, Oct. 2003.
- [26] X. L. Bao, G. Ruvio, M. J. Ammann, and M. John, "A novel GPS patch antenna on a fractal high-impedance surface substrate," *IEEE Antennas Wireless Propag. Lett.*, vol. 5, pp. 323-326, 2006.
- [27] H. Mosallaei, and K. Sarabandi, "Antenna miniaturization and bandwidth enhancement using a reactive impedance substrate," *IEEE Trans. Antennas Propag.*, vol. 52, no. 9, pp. 2403-2414, Sep. 2004.
- [28] R. F. J. Broas, D. F. Sievenpiper, and E. Yablonovitch, "A high-impedance ground plane applied to a cellphone handset geometry," *IEEE Trans. Microw. Theory Tech.*, vol. 49, no. 7, pp. 1262-1265, July 2001.
- [29] A. P. Feresidis, G. Goussetis, S. Wang, and J. C. Vardaxoglou, "Artificial magnetic conductor surfaces and their application to low-profile high-gain planar antennas," *IEEE Trans. Antennas Propag.*, vol. 53, no. 1, pp. 209-215, Jan. 2005.
- [30] H. Li, S. Khan, J. Liu, and S. He, "Parametric analysis of Sierpinski-like fractal patch antenna for compact and dual band WLAN applications," *Microw. Opt. Technol. Lett.*, vol. 51, no. 1, pp. 36-40, Jan. 2009.
- [31] M. Hosseini and S. Bashir, "A novel circularly polarized antenna based on an artificial ground plane," *Progress Electromagn. Research Lett.*, vol. 5, pp. 13-22, 2008.
- [32] S. Malisuwan, J. Sivaraks, N. Madan, and N. Suriyakrai, "Design of microstrip patch antenna for Ku-band satellite communication applications," *Int. J. Comput. Commun. Eng.*, vol. 3, no. 6, pp. 413-416, Nov. 2014.
- [33] J. Wargo, *Unlicensed 24 GHz Point to Point Wireless Backhaul Option*, May 2010. [Online]. Available: <http://www.aowireless.com>
- [34] SAF Tehnika JSC, *Highspeed Internet Provider Selects SAF Freemile 24 GHz to Extend Its Network in Hawaii*. Jun. 2012. [Online]. Available: <http://www.openpr.com/news/226290/>
- [35] F. Alimenti, P. Mezzanotte, G. Tasselli, A. Battistini, V. Palazzari, and L. Roselli, "Development of low-cost 24-GHz circuits exploiting system-in-package SiP approach and commercial PCB technology," *IEEE Trans. Compon. Packag. Manuf. Technol.*, vol. 2, no. 8, pp. 1265-1274, 2012.
- [36] M. Poggiani, F. Alimenti, P. Mezzanotte, M. Virili, C. Mariotti, G. Orecchini, and L. Roselli, "24-GHz patch antenna array on cellulose-based materials for green wireless internet applications," *IET Sci. Meas. Technol.*, vol. 8, no. 6, pp. 342-349, 2014.
- [37] H. Y. Chen, T. H. Lin, and P. K. Li, "Fast design of Jerusalem-cross parameters by equivalent circuit model and least-square curve fitting technique," *Appl. Comput. Electromagn. Soc. J.*, vol. 31, no. 4, pp. 455-467, 2016.

- [38] H. Y. Chen and S. H. Wen, "An Empirical formula for resonant frequency shift due to Jerusalem-cross FSS with substrate on one side," *Appl. Comput. Electromagn. Soc. J.*, submitted, Nov. 16, 2016.



**Shu-Huan Wen** was born in Taiwan, in 1991. He received the B.S. degree in Electronic Engineering from Oriental Institute of Technology in 2013. He is currently working toward the Ph.D. degree in Communications Engineering at Yuan Ze University, Taiwan. His research interests include

patch antenna design, frequency selective surfaces, EM field measurement, and computational electromagnetics.



**Hsing-Yi Chen** was born in Taiwan, in 1954. He received the B.S. and M.S. degrees in Electrical Engineering in 1978 and 1981 from Chung Yuan Christian University and National Tsing Hua University, respectively. He received the Ph.D. degree in Electrical Engineering

from University of Utah, Salt Lake City, Utah in 1989. He joined the faculty of the Department of Electrical

Engineering, Yuan Ze University, Taiwan, in September 1989. He was the Chairman of Electrical Engineering from 1996 to 2002, the Chairman of Communications Engineering from 2001 to 2002, the Dean of Engineering College from 2002 to 2006, the Dean of Electrical and Communication Engineering College from 2006 to 2012, and the Dean of Research and Development Office from 2012 to 2013. Currently, he is the Dean of General Affairs Office, Yuan Ze University. His current interests include electrostatic discharge, electromagnetic scattering and absorption, waveguide design, radar systems, electromagnetic compatibility and interference, bio-electromagnetics, electromagnetic radiation hazard protection, and applications of frequency selective surface.

He is a member of Phi Tau Phi. He was also a member of the editorial board of the *Journal of Occupational Safety and Health* from 1996 to 1997. He was elected an Outstanding Alumnus of the Tainan Second High School in 1995. He has been the recipient of numerous awards including the 1990 Distinguished Research, Service, and Teaching Award presented by the Yuan Ze University, the 1999 and 2002 YZU Outstanding Research Award, and the 2005 Y. Z. Hsu Outstanding Professor Award for Science, Technology & Humanity Category. He was awarded Chair Professor by Far Eastern Y. Z. Hsu Science and Technology Memorial Foundation in 2008. His name is listed in *Who's Who in the World* in 1998.